



Protective effects of probiotics against methotrexate-induced intestinal toxicity in the mice model

KSENIA S. STAFEEVA¹; NATALIA A. SAMOYLOVA¹; OLGA A. KARANDEEVA¹; VERONIKA V. NESTEROVA¹;
KIRILL A. STARODUBTSEV¹; EVGENY V. MIKHAILOV²; ILYA O. KRUTOV²; EVGENY S. POPOV³; NATALIA S. RODIONOVA⁴;
ANASTASIA V. KOKINA^{1,5}; ARTEM P. GUREEV^{1,5,*}

¹ Department of Genetics, Cytology and Bioengineering, Biomedical faculty, Voronezh State University, Voronezh, 394018, Russia

² Experimental Pharmacology Department, All-Russian Scientific Research Veterinary Institute of Pathology of Pharmacology and Therapy, Voronezh, 394087, Russia

³ Department of Service and Restaurant Business, Voronezh State University of Engineering Technology, Voronezh, 394000, Russia

⁴ Department of Quality Management, Hospitality and Tourism, Voronezh State University of Engineering Technology, Voronezh, 394000, Russia

⁵ Laboratory of Metagenomics and Food Biotechnology, Voronezh State University of Engineering Technology, Voronezh, 394000, Russia

Key words: Small intestine, Mitochondrial DNA, Mitochondria, Il1b, Trp53bp1

Abstract: Objective: The objective of this study was to determine the level of methotrexate (MTX) toxicity in the intestines of mice and to evaluate the protective effect of probiotics composed of *Streptococcus*, *Bifidobacterium*, and *Lactobacillus* species on intestinal cells during MTX treatment. **Methods:** Mice were divided into three groups: control, MTX group (received MTX injections), and MTX + probiotics group (received MTX injections along with a diet containing probiotics). Morphological and histological changes, the level of mitochondrial DNA (mtDNA) damage, the level of lipid peroxidation products, and gene expression in the mice's small intestine were assessed. **Results:** We demonstrated that intraperitoneal MTX injections significantly increased mtDNA damage in the liver ($p < 0.001$), small intestine ($p < 0.001$), and blood of mice ($p < 0.01$). MTX elevated the quantity of lipid peroxidation products in the liver and small intestine, indicating its strong prooxidative properties. MTX induced structural changes in the mice's intestines, characterized by leukocytic infiltration of tissues. Probiotic therapy in mice partially mitigated the morphological and histological changes in the small intestine induced by MTX, reduced oxidative stress, and promoted increased expression of quinone oxidoreductase 1 (*Nqo1*), which participates in both cell protection against oxidative stress and drug/xenobiotic detoxification. Probiotics prevented the upregulation of the pro-inflammatory cytokine IL-1b in the small intestine and induced increased expression of genes associated with the Nuclear factor erythroid 2-related factor 2/Antioxidant response element (*Nrf2/ARE*) pathway, an important mechanism of cell protection. **Conclusions:** Probiotics can be considered an effective approach to reducing the toxicity of MTX during psoriasis or cancer treatment.

Abbreviations

MTX	Methotrexate
mtDNA	Mitochondrial DNA
ROS	Reactive oxygen species
GSH	Glutathione
TNF- α	Tumor necrosis factor alpha
RA	Rheumatoid arthritis

CIM	Chemotherapy-induced acute small intestinal mucositis
DC	Diene conjugates
MDA	Malondialdehyde
DHFR	Dihydrofolate reductase
NOS	Nitric oxide synthases
Nrf2	Nuclear factor erythroid 2-related factor 2
HO-1	Heme oxygenase 1
NO	Nitric oxide
IL-1b	Interleukin 1beta
Nrf2/ARE	The Nuclear factor erythroid 2-related factor 2/Antioxidant response element

*Address correspondence to: Artem P. Gureev, gureev@bio.vsu.ru
Received: 10 September 2024; Accepted: 28 November 2024;
Published: 24 January 2025

Doi: 10.32604/biocell.2024.058339

www.techscience.com/journal/biocell



Copyright © 2025 The Authors. Published by Tech Science Press.

This work is licensed under a Creative Commons Attribution 4.0 International License, which permits unrestricted use, distribution, and reproduction in any medium, provided the original work is properly cited.

NQO1	Quinone oxidoreductase 1
BRCA1	breast cancer susceptibility gene 1
OGG1	Oxoguanine glycosylase 1
MTS	Mitochondrial targeting signal

Introduction

Currently, cancer is the second leading cause of death worldwide [1]. One of the main methods of treating oncological diseases is chemotherapy using cytotoxic drugs that inhibit cell proliferation, induce oxidative stress, disrupt DNA structure, and interfere with mechanisms involved in DNA replication and cell division [2]. An important limitation of chemotherapy is that the drugs used have a non-targeted effect and are highly toxic not only to tumor cells but also to normal proliferating tissues [3]. Many anticancer drugs impair mitochondrial functions, subsequently affecting healthy tissues in the body. For instance, acrolein induces mitochondrial stress by increasing levels of reactive oxygen species (ROS) production and reducing the expression of catalase or glutathione (GSH) [4]. Adriamycin elevates tumor necrosis factor alpha (TNF- α) levels specifically in the hippocampal region of animals, which disrupts mitochondrial complex I substrate and thereby impairs mitochondrial respiration and exacerbates oxidative stress [5]. Cisplatin damages mitochondrial DNA (mtDNA), reduces antioxidant expression, and disrupts gut microbiome homeostasis [6,7].

One of the most widely used drugs is methotrexate (MTX), which finds application in the treatment of various rheumatic conditions, juvenile idiopathic arthritis, psoriasis, primary biliary cirrhosis of the liver, and asthma [8,9]. Additionally, MTX is used as standard prophylaxis for graft vs. host reactions [10], and as a therapeutic agent for dermatological conditions. MTX exhibits efficacy in treating fungal infections, lichen planus, and sarcoidosis. Moreover, it proves effective in certain cancers such as lymphoma, osteosarcoma, various forms of leukemia, breast cancer, and bladder cancer [11]. Five-year survival rates for osteosarcoma have increased to 70%–80% with the introduction of drug combinations of MTX + doxorubicin + cisplatin in addition to surgical approaches [12]. Patients with rheumatoid arthritis (RA) who received MTX were shown to have a 28% reduced risk of overall mortality. The risk of cardiovascular disease in RA was reduced by 28% and the risk of rheumatoid lung disease was reduced by 56% [13]. Studies indicate that discontinuation of MTX within the first year of RA treatment correlates with higher mortality rates among patients [14].

Like other antitumor drugs, MTX has a number of side effects, including hepatotoxicity, bone marrow suppression, and, less commonly, hypersensitivity pneumonitis and opportunistic infections [15]. Furthermore, MTX can increase lipid peroxidation in mitochondrial membranes and reduce levels of GSH and catalase, resulting in oxidative stress. It can also impair mitochondrial respiration independently of GSH [16].

An important side effect of MTX is its gastrointestinal tract toxicity, which manifests as inhibition of growth and

regenerative activity of intestinal epithelium and mucous membranes, resulting in intestinal mucositis. MTX is commonly used to induce acute chemotherapy-induced acute small intestinal mucositis (CIM) in rats [17,18]. There are reports suggesting that several drugs can mitigate the hepatotoxicity caused by MTX. For instance, silybinin has been demonstrated to reduce liver damage induced by MTX by enhancing antioxidant activity [19]. Similarly, fasudil has been found to restore the oxidant-antioxidant balance, alleviate liver inflammation, and enhance the anti-apoptotic capacity of the liver following MTX-induced damage [20]. However, comparatively less attention has been paid to preventing gastrointestinal tract damage during MTX therapy.

One potential approach to mitigate gastrointestinal tract damage during chemotherapy involves the utilization of probiotics, live microorganisms primarily comprising strains of *Lactobacillus* and *Bifidobacterium* species [21]. Probiotic strains have been shown to exhibit anti-tumor effects within the intestine. In several studies, it has been reported that probiotics can induce apoptosis in colorectal cancer cells by modulating key apoptosis-related signaling pathways. Additionally, the exopolysaccharides secreted by these probiotic bacteria have been found to inhibit the proliferation of cancer cells [22]. Probiotics have been shown to reduce inflammation in the intestines caused by Celecoxib therapy. Probiotic mixtures have been shown to alleviate intestinal inflammation induced by Celecoxib therapy [23], and reduce the risk of mucositis during platinum-based drug therapy [24], as well as during treatment with daunorubicin, vincristine [25], and 5-fluorouracil [26]. Probiotic mixtures have also been found to reduce diarrhea during irinotecan therapy [27] and radiation therapy [28]. Indeed, the gut microbiota can serve as an additional factor that enhances the anti-tumor therapeutic effect. It has been shown that administering bacterial preparations to mice reduces the inflammatory reactions caused by MTX and modulates macrophage polarization [29].

In this study, we aimed to evaluate the mitochondrial toxicity of MTX across multiple organs in mice, with a primary emphasis on the gastrointestinal tract. Furthermore, we aimed to explore the protective mechanism of probiotic mixtures comprising bacteria from the *Streptococcus*, *Bifidobacterium*, and *Lactobacillus* genera on intestinal cells in the context of MTX-induced damage.

Materials and Methods

Animals

Two-month-old male C57BL/6 mice weighing 18 g obtained from the “Stolbovaya” breeding facility (Moscow region, Russia) were used in the experiment. The rearing, housing, and killing of mice was performed in accordance with the rules established by the Ethical Committee for Biomedical Research of Voronezh State University (Section of Animal Care and Use, Minutes 42-03, 08 October 2020). Animals were kept 4–6 mice each in a plastic cage (30 cm \times 20 cm \times 18 cm). Mice were maintained under standard conditions (25°C, 12-h light/dark cycle, relative humidity >40%). They had *ad libitum* access to standard laboratory diet and drinking water.

In vitro experiment design. Isolation of mitochondria from mouse liver

The buffer used for mitochondria isolation contained the following components: 225 mM mannitol (Dia-M, TC1513.100 gm, Moscow, Russia), 75 mM sucrose (Panreac, 141621, Barcelona, Spain), 1 mM ethylene glycol tetraacetic acid (EGTA) (Applichem, A5097, Darmstadt, Germany), and 20 mM HEPES (Bioclot GmbH, P5455-KG, Aidenbach, Germany). All components were dissolved in distilled water. The pH of the solution was adjusted to 7.4 by adding dry KOH.

Animals were sacrificed by rapid cervical dislocation followed by decapitation without the use of anesthetics. The liver was homogenized using a Bioprep-6 laboratory homogenizer (Allsheng, Allsheng-AS-13020-00, Hangzhou, China) in 15 mL of buffer, which additionally contained bovine serum albumin (BSA) (Dia-M, BSA.0010, Moscow, Russia) at a concentration of 6 mg/mL. All manipulations with mitochondria were performed on ice, and centrifugation was done in a cooled centrifuge at a temperature of 4°C. The obtained homogenate was transferred to a chilled centrifuge tube and brought to the required volume with buffer, then centrifuged for 5 min at 500 g. The supernatant was collected and brought to the desired volume with a buffer. Then, centrifugation was performed for 10 min at 10,000 g. The resulting pellet was carefully resuspended in 1 mL of buffer cooled to 4°C and subjected to a second centrifugation for 10 min at 10,000 g. The pellet containing mitochondria was resuspended in 50 µL of buffer. Protein concentration was measured using the Lowry method [30] on a Hitachi U-2900 spectrophotometer (Hitachi, RS-232C, Tokyo, Japan).

Each sample contained 10 mg of protein. MTX solution was added to the samples to achieve a final concentration of 12.5 µg/mg, 25 µg/mg, and 37.5 µg/mg of mitochondrial protein, which was previously dissolved in the buffer for mitochondrial isolation. Control samples were added to the buffer for mitochondrial isolation in an equivalent volume. All samples were incubated in a shaker at 25°C for 30 min. Following the incubation, DNA was extracted from intact mitochondria, and the concentration of diene conjugates (DC) and malondialdehyde (MDA) was evaluated as markers of lipid peroxidation.

In vivo experiment design

The control group of mice ($n = 6$) was kept under standard conditions, received a standard laboratory diet (maintenance diet for rats and mice, Altromin Spezialfutter GmbH, Lage, Germany), and was injected with a physiological saline solution from day 13 to day 18. The MTX group ($n = 8$) received a standard diet throughout the entire experiment and were injected with MTX (commercially available product "Methotrexate-ebewe" from FAREVA Unterach GmbH, Unterach am Attersee, Austria) at a concentration of 5 mg/kg/day for 6 days (from day 13 to day 18). The MTX + probiotics group ($n = 8$), who also received injections of MTX at a concentration of 5 mg/kg for 6 days (from day 13 to day 18), were given probiotics mixed with the standard diet (13 g of probiotics per 56 g of diet) for the entire 18-day duration of the experiment (Fig. 1). Probiotic weight (grams)

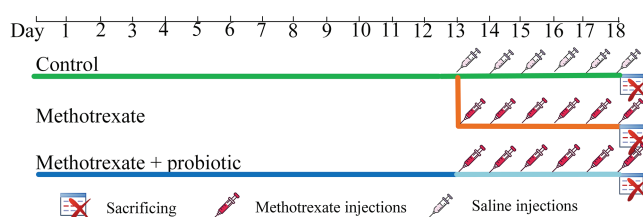


FIGURE 1. *In vivo* experiment design.

refers to wet weight. The daily consumption of food was evaluated. The average daily consumption of probiotics was 0.64 g of probiotics per gram of mouse body weight. The probiotics used contained the following strains: *Streptococcus thermophiles* (B-8328), *Bifidobacterium bifidum* (AC-1579), *B. longum* (AC-1257), *B. adolescentis* (AC-1245), *Lactobacillus rhamnosus* (B-8238), *L. acidophilus* (B-5097), *L. plantarum* (B-3962), *L. fermentum* (B-2875). The cultivated biomass had a concentration of active cells of not less than 10^9 CFU/mL, titratable acidity was 80–100°T, pH 4.61–4.65 (produced by Voronezh State University of Engineering Technologies, Voronezh, Russia). Biomass growth was carried out on skim milk in the temperature range of 38°C–40°C, the standard cultivation time was 8–10 h. Each mouse was weighed daily, and on the 18th day of the experiment, the mice were sacrificed. Organs and blood were collected, frozen in liquid nitrogen, and then stored at –80°C for further DNA and RNA extraction, histological analysis, as well as evaluation of the level of lipid peroxidation products.

DNA and RNA extraction

DNA extraction from different organs and blood was carried out using the Proba-GS kit (DNA-Technology, P-003/1, Moscow, Russia) according to the protocol. The ExtractRNA commercial kit (Evrogen, BC032, Moscow, Russia) was used for RNA extraction from the samples according to the protocol.

Estimation of gene expression level

For reverse transcription, the Reverta-L kit (Amplise, K3-4-100, Moscow, Russia) was used according to the provided protocol. Quantitative PCR analysis was performed using the Bio-Rad CFX96™ Real-Time System instrument (Bio-Rad, 1845096, Hercules, CA, USA). The reaction mixture (20 µL) included: 4 µL 5X qPCRmix-HS SYBR (Evrogen, PK147L, Moscow, Russia), 1 µL mixture of forward and reverse primers, 1 µL of the DNA sample, and 14 µL of mQ water. The PCR cycling conditions were as follows: total denaturation at 95°C for 3 min, denaturation at the beginning of the cycle at 95°C for 30 s, primer annealing at 59°C for 30 s, and elongation at 72°C for 30 s; the number of cycles was 45. The final extension step was performed at 72°C for 5 min. *Gapdh* was used as a reference. The primer sequences are presented in Table 1.

Measuring the mtDNA damage level

To assess the level of mtDNA damage, a long-range PCR was employed using the Encycle polymerase kit (Evrogene, PK002S, Moscow, Russia) on the CFX96™ Real-Time System thermocycler (Bio-Rad, 1845096). The principle of the method is that mtDNA damage hinders the activity of

TABLE 1

Primer sequences for assessing gene expression levels

Gene name	Forward primer sequence 5' → 3'	Reverse primer sequence 3' → 5'	Accession number	References
<i>Nfe2l2</i>	CTCTCTGAACTCCTGGACGG	GGGTCTCCGTAAATGGAAG	NM_010902.4	[7]
<i>p62</i>	GCCAGAGGAACAGATGGAGT	TCCGATTCTGGCATCTGTAG	NM_011018.3	[7]
<i>Pink1</i>	GAGCAGACTCCAGTTCTCG	GTCCCACTCCACAAGGATGT	NM_026880.2	[7]
<i>Il1b</i>	TTGACGGACCCAAAAGATG	AGAAGGTGCTCATGTCTCA	NM_008361.4	[31]
<i>Il6</i>	CGGAAGAGGAGACTTCACAGAG	CATTTCCACGATTTCCAGAG	NM_031168.2	[31]
<i>Tnf</i>	TATGGCTCAGGGTCCAATC	GGAAAGCCATTTGAGTCCT	NM_013693.3	[31]
<i>Ptgs2</i>	AGTCCGGGTACAGTCACACTT	TTCCAATCCATGTCAAACCGT	NM_011198.5	[31]
<i>Brcal</i>	AGGTGATTGCAGTGTGAGAGA	GTATCCCGATGCCTCTCTC	NM_009764.3	[7]
<i>Ogg1</i>	GAGACGACAGCCAGGTGTGAG	CCGTTCCACCATGCCAGTA	NM_010957.5	[7]
<i>Trp53bp1</i>	GAAGGAAAGCACAGATGAGGATT	CTAGAGGTTTCTGCACGCTG	NM_013735.5	[7]
<i>Nqo1</i>	GGACATGAACGTCATTCTCT	TTCTTCTTCTGCTCCTCTTG	NM_008706.5	[32]
<i>Gapdh</i>	GGCTCCCTAGGCCCTCCTG	TCCCAACTCGGCCCAACA	NM_001289726.1	[7]

DNA polymerase, resulting in a reduced rate of product accumulation. The primer sequences are presented in Table 2.

Each PCR reaction contained 1 × Encyclo-polymerase, 1 × Encyclo-buffer, 0.2 mM of each dNTP (all from “Evrogen”, Moscow, Russia), 1 × SYBR GreenMasterMix (Bio-Rad, 1725270, California, USA), and a mixture of forward and reverse primers in a total volume of 20 µL. The PCR cycling conditions were as follows: total denaturation at 95°C for 3 min; 35 cycles: denaturation at the beginning of the cycle at 95°C for 30 s, primer annealing at 59°C for 30 s, elongation at 72°C for 4 min and 30 s.

The difference in Cq values (ΔCq) for the control and experimental long fragments was compared with the ΔCq for the control and experimental short fragments. The number of additional damages in mtDNA was calculated per 10 kb using the following formula:

$$\text{Lesions} = (1 - 2^{-(\Delta_{\text{long}} - \Delta_{\text{short}})}) \times (10,000(\text{bp}) / \text{fragment length (bp)})$$

where $\Delta_{\text{long}} = Cq \text{ control} - Cq \text{ experiment}$ for the long fragment and $\Delta_{\text{short}} = Cq \text{ control} - Cq \text{ experiment}$ for the short fragment.

Histological studies and measurement of intestinal length

After sacrificing the mice, the length of the mouse intestine was measured. The length of the small intestine was considered from the stomach to the cecum. The length of the colon was evaluated from the cecum to the anus. For morphological studies of the small intestine, tissue samples were fixed in a 10%–12% solution of neutral formalin HistoSafe® (Biovitrum, B06-003/5, Moscow, Russia). Subsequently, the intestine tissue was dehydrated through increasing concentrations of ethyl alcohol and embedded in histological paraffin “Histomix” (Biovitrum, 247, Moscow, Russia). Sections with a thickness of 3–5 µm were obtained from paraffin blocks using a rotary microtome MPS-2 (Tochmedpribor, 00460, Kharkov, Ukraine). The sections were stained using classical histological methods, such as hematoxylin and eosin.

Deparaffinization of histological sections was performed in three “batches” of O-xylene (ChDA) (Ekos-1, 1330-20-7, Moscow, Russia) for three minutes each, followed by rehydration in four “batches” of alcohol with decreasing concentrations. This was followed by rinsing in distilled water for 20 s, after which the histological sections were stained with Harris hematoxylin (Biovitrum 05-001,

TABLE 2

Primer sequences for measuring mtDNA damage

Fragment name	Forward primer sequence 5' → 3'	Reverse primer sequence 3' → 5'	Fragment length (bp)	References
1 long	TAAATTTTCGTGCCAGCCACC	ATGCTACCTTTGCACGGTCA	1739	[7]
2 long	ACGAGGGTCCAACCTGTCTCTTA	CCGGCTGCGTATTCTACGTT	1326	[7]
3 long	CTAGCAGAAACAAACCGGGC	TTAGGGCTTTGAAGGCTCGC	1675	[7]
4 long	TCATTCTTCTACTATCCCCAATCC	TGGTTTGGGAGATTGGTTGATG	1942	[7]
5 long	CCCCAATCCCTCCTTCCAAC	GGTGGGGAGTAGCTCCTTCTT	1732	[7]
6 long	AAGAAGGAGCTACTCCCCACC	GTTGACACGTTTTACGCCGA	1308	[7]
Short	ACGAGGGTCCAACCTGTCTCTTA	AGCTCCATAGGGTCTTCTCGT	97	[7]

Moscow, Russia) for 5 min. The stained sections were then washed under running water for 30 min. To stain eosinophilic structures, the histological sections were rinsed in three batches of distilled water and immersed in a wide-mouth flask with water-alcohol eosin (Labiko, LLC Labiko, E-013/1000, Saint Petersburg, Russia) for 20 s. After staining the eosinophilic structures, they were rinsed in distilled water for 30 s, quickly “dried” on filter paper, and then differentiated in increasing concentrations of alcohol: 70°, 80°, and 96° for 3 s each, with a “delay” of the histological sections in 100° alcohol for 2 min. After treatment with 100° alcohol, the histological sections were placed in a “batch” of carbol xylene for 2 min, followed by transfer to two “batches” of O-xylene for 5 min each. The “mounting” of the stained histological sections was performed using Canada balsam (Panreac, 251179.1611, Barcelona, Spain). Evaluation of tissue architecture was conducted using light microscopy with a Biomed 4 microscope (Biomed, 00000023514, Moscow, Russia) [33].

Assessment of the level of lipid peroxidation products

To quantify the levels of MDA and DC, tissue samples were homogenized in 2 mL of phosphate buffer solution. The resulting homogenates underwent centrifugation at 500 g for 5 min at 4°C, and the supernatants were collected for subsequent analysis.

MDA concentration was determined as follows: 400 μ L of the supernatant was aliquoted into test tubes, followed by the addition of 600 μ L of 20% trichloroacetic acid (Lenreactiv, 180324, St. Petersburg, Russia). The mixture was then incubated at cold temperatures for 30 min with intermittent agitation every 10 min. Subsequently, the samples were centrifuged at 10,000 g for 10 min at 4°C. Next, 300 μ L of the resulting supernatant was transferred to fresh test tubes, to which 3 mL of trichloroacetic acid and 1 mL of 0.8% thiobarbituric acid (Lenreactiv, 180160, St. Petersburg, Russia) were added. The contents were thoroughly mixed and incubated in a water bath for 40 min, followed by cooling. The MDA levels were measured spectrophotometrically at wavelengths of 530 and 580 nm [34].

The calculations were performed using the following formula: $C_{\text{MDA}} = (E_{530} - E_{580}) / (\epsilon \cdot L \cdot m)$, where C_{MDA} —concentration of MDA (mmol/mg), E_{530} —the optical density at a wavelength of 530 nm, E_{580} —the optical density at a wavelength of 580 nm, ϵ —the molar extinction coefficient ($\text{mM}^{-1} \cdot \text{cm}^{-1}$), L —the optical path length (cm), m —mass of the sample (mg).

The determination of conjugated dienes (CD) concentration was carried out as follows: 125 μ L of the prepared supernatant was combined with 125 μ L of physiological solution (MOSPHEARM, 005263/07, Moscow, Russia). To this mixture, 1.5 mL each of heptane (Lenreactiv, 443043, St. Petersburg, Russia) and isopropyl alcohol (Dia-M, 3827.1000, Moscow, Russia) were added in test tubes. The resulting solution was then centrifuged for 10 min at 3000 g at 4°C. Subsequently, the supernatant was carefully transferred to fresh test tubes, followed by the addition of distilled water and vigorous mixing. After phase separation, the upper phase was collected, and 500 μ L of 96% ethanol was added. The determination of conjugated

dienes level was conducted spectrophotometrically at a wavelength of 233 nm. The calculation was conducted using the formula:

$C_{\text{CD}} = (V_{\text{total}} \cdot D \cdot 10^6) / (L \cdot \epsilon \cdot m \cdot V_{\text{add}})$, where C_{CD} —the concentration of DC (mmol/mg), V_{total} —the total volume of the sample (μ L), D —optical density, ϵ —the molar extinction coefficient ($\text{mM}^{-1} \cdot \text{cm}^{-1}$), V_{add} —the volume of supernatant taken for analysis (μ L), L —the optical path length (cm), m —a mass of the sample (mg) [7].

The statistical analysis

The results obtained during the experiment are presented as mean values \pm standard error. The statistical analysis was performed using the Statistica 12.0 software package (StatSoft, Inc., USA). The normality of the data distribution was determined using the Shapiro-Wilk test. The Kruskal-Wallis analysis of variance was used to determine the level of significance. A statistically significant difference was considered to be an adjusted p -value of ≤ 0.05 .

Results

The effect of MTX on liver mitochondria in vitro

We investigated the toxicity of MTX on isolated liver mitochondria *in vitro*. Our findings reveal that MTX significantly amplifies oxidative damage to mtDNA, particularly notable at a concentration of 37.5 μ g/mg protein (a fivefold increase, $p < 0.001$), while no statistically significant elevation in damage was noted at lower concentrations (Fig. 2A). Additionally, MTX notably stimulates lipid peroxidation within the mitochondria. A more than threefold increase in DC concentration was observed upon MTX addition at a concentration of 25 μ g/mg protein ($p < 0.01$) (Fig. 2B). Consistent outcomes

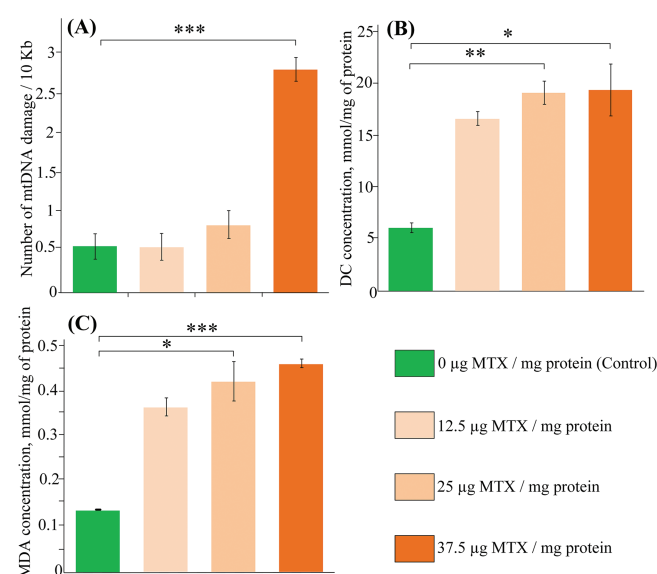


FIGURE 2. The effect of methotrexate (MTX) on (A) mitochondrial DNA (mtDNA) damage, (B) concentration of diene conjugates, (C) levels of malondialdehyde upon the addition of different concentrations of MTX to isolated liver mitochondria ($n = 3$). Differences between groups are statistically significant: * $p < 0.05$, ** $p < 0.01$, *** $p < 0.001$ (Kruskal-Wallis test).

were obtained in the assessment of MDA concentration, revealing a threefold rise in lipid peroxidation products subsequent to the addition of MTX at a concentration of 25 µg/mg protein ($p < 0.05$) (Fig. 2C).

The effect of MTX on body weight changes in mice

The use of probiotics for 10 days had no effect on the body weight of the mice, and no statistically significant differences were found compared to the control group. Starting from the 11th day of the experiment, two groups of mice received daily injections of MTX at a concentration of 5 mg/kg/day. On the 2nd day after the start of the injection course, the body weight of mice receiving only food and MTX injections was 15% lower than that of the control mice ($p < 0.05$). Furthermore, mice receiving MTX injections continued to experience a decrease in body weight. By the 6th day of injections, the body weight of mice receiving only MTX was 32% lower than that of the control group ($p < 0.01$). It is worth noting that the MTX-induced reduction in body weight was also observed in mice receiving probiotics, but the differences compared to the control group were not statistically significant (Fig. 3).

The impact of MTX on the amount of mtDNA damage in different organs

We analyzed the influence of MTX on the amount of damage in different sections of the gastrointestinal tract. There was no increase in mtDNA damage observed in the stomach and colon after the course of MTX injections (Fig. 4A,B). However, MTX injections resulted in an 82% increase in mtDNA damage in the small intestine compared to the control group ($p < 0.001$). Additionally, mice that received pre-treatment with probiotics had 26% less damage compared to mice that only received MTX injections (Fig. 4C). However, probiotics did not have any effect on mtDNA damage in the cerebral cortex, heart, and lung (Fig. 4D–F).

Among all the internal organs studied, the liver was most susceptible to MTX-induced mtDNA damage (+98% compared to control, $p < 0.001$). Probiotics did not have an impact on the amount of mtDNA damage in the liver (Fig. 4G). However, in the kidneys of mice that received simultaneous treatment with MTX and probiotics, the

amount of mtDNA damage was 27% lower than in the control group ($p < 0.001$) (Fig. 4H). It is worth noting that MTX caused an increase in the level of mtDNA damage in the blood (+86%, $p < 0.01$). Treatment with probiotics did not affect the amount of mtDNA damage in the blood (Fig. 4I). Probiotics partially reduced the level of damage in the small intestine (–26%, $p < 0.05$).

The effect of MTX and probiotics on the levels of lipid peroxidation products

Since the small intestine and liver exhibited the highest levels of mtDNA damage, we further assessed the levels of lipid peroxidation products in these organs. The level of MDA in the livers of mice receiving MTX injections was twofold higher than that of control mice, but the differences were not statistically significant ($p = 0.053$) (Fig. 5A). However, the level of DC in the livers of mice receiving MTX injections was 67% higher than that of control mice ($p < 0.05$) (Fig. 5B). In mice receiving simultaneous treatment with MTX and probiotics, there was no statistically significant increase in the levels of both MDA and DC compared to the control group.

In the small intestine, there was also a tendency towards increased levels of MDA and DC after MTX injections (+50% and +107%, respectively). However, probiotics in the small intestine stimulated a reduction in DC levels (–45%) and MDA levels (–47%), which were approximately similar to the values observed in control mice (Fig. 5C,D).

Effect of MTX and probiotics on the level of gene expression

In the small intestine of mice receiving MTX injections, the expression of *Il1b* was increased by 10-fold compared to control mice ($p < 0.05$). Although the expression of *Il1b* was also increased 5-fold in the mice receiving MTX and probiotics, the differences with control were not statistically significant. No differences were found in the expression levels of other pro-inflammatory cytokines (*Il6*, *Tnf*) and the inflammation marker *Ptgs2*. MTX stimulated an increase in the expression of the *Nfe2l2* gene in the small intestine of mice, but a statistically significant 5-fold increase in *Nfe2l2* expression was only observed in mice receiving probiotics treatment in addition to MTX ($p < 0.05$).

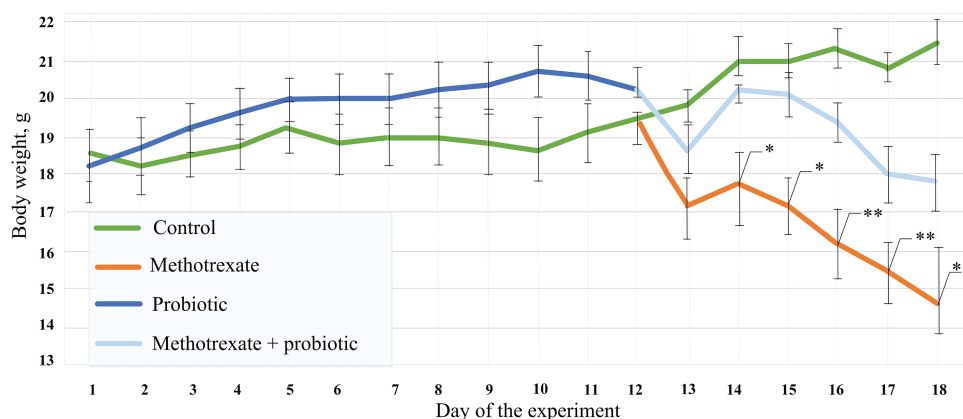


FIGURE 3. The effect of methotrexate (MTX) and probiotics on the dynamics of body weight throughout the entire duration of the experiment. The control group of mice ($n = 6$), the MTX group ($n = 8$), and the MTX + probiotics group ($n = 8$). The differences between the control group and the group of mice receiving MTX injections were statistically significant: * $p < 0.05$, ** $p < 0.01$ (Kruskal-Wallis test).

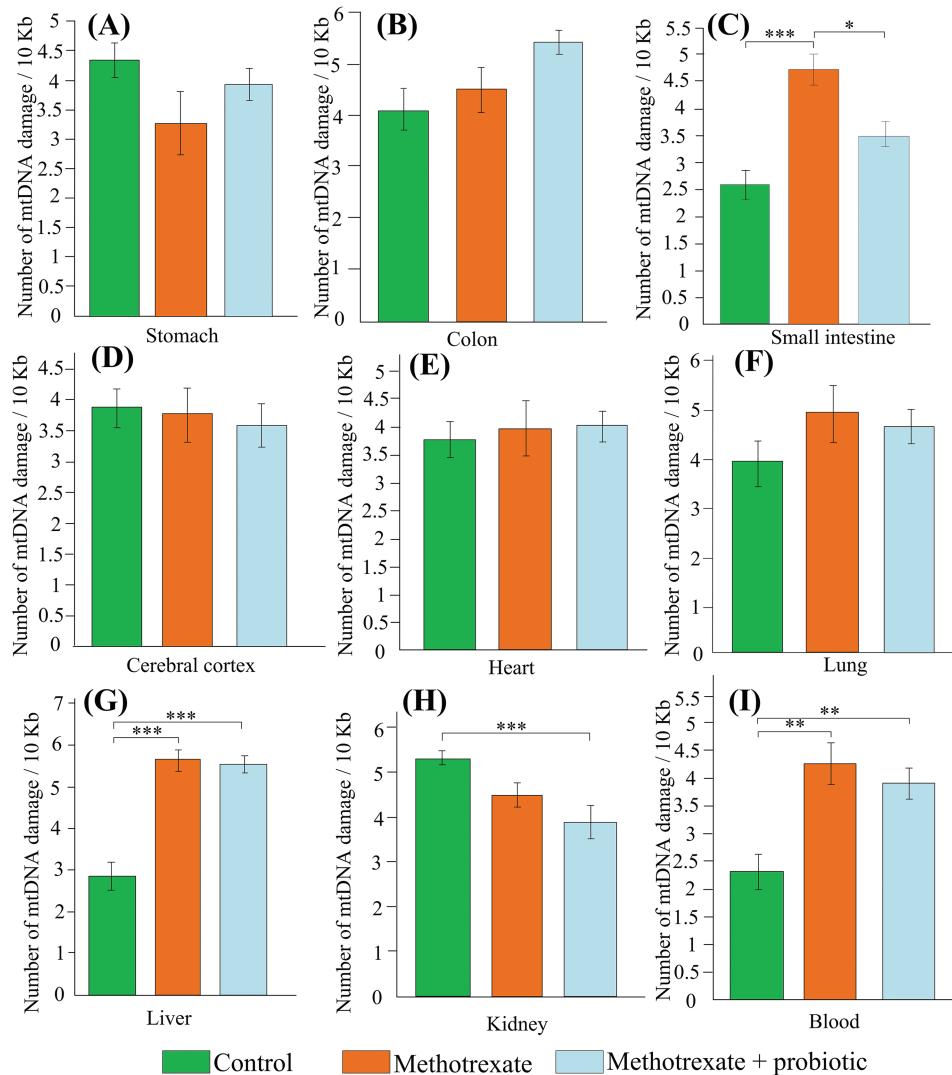


FIGURE 4. The effect of methotrexate (MTX) and probiotics on the amount of mtDNA damage in the stomach (A), colon (B), small intestine (C), cerebral cortex (D), heart (E), lung (F), liver (G), kidney (H), blood (I) of mice. The control group of mice (n = 6), the MTX group (n = 8), and the MTX + probiotics group (n = 8). Differences between groups are statistically significant: * $p < 0.05$, ** $p < 0.01$, *** $p < 0.001$ (Kruskal-Wallis test).

In mice receiving simultaneous treatment with MTX and probiotics, the expression of genes involved in DNA repair, including partially mtDNA repair, was increased. This includes the genes *Ogg1* (increased 3-fold) and *Brca1* (increased 6-fold) (both $p < 0.05$ compared to control). Mice receiving probiotics and MTX showed a three-fold increase in *Trp53bp1* expression compared to mice receiving only MTX injections ($p < 0.05$). In the small intestine of mice in the MTX + probiotics group, the expression of *Nqo1* was increased 12-fold compared to control ($p < 0.01$) and 5-fold compared to the group receiving MTX injections only ($p < 0.05$). There were no changes observed in the expression of genes involved in mitophagy (*p62* and *Pink1*) (Fig. 6).

Histological analysis and differences in intestinal length

Measurement of the small intestine and colon length was conducted to assess the severity of inflammatory processes induced by MTX. We found that the mean length of the small intestine in the control group of mice was 35.56 ± 1.22 cm (Fig. 7A,C). In the group of mice receiving MTX

injections, the mean length of the small intestine was 26.37 ± 1.1 cm, which was significantly shorter than in the control group ($p < 0.001$) (Fig. 7A,D). In the group of mice receiving MTX and probiotics, the length of the intestine was 30.72 ± 1.2 cm (Fig. 7A,E). The mean length of the colon did not differ between the experimental groups of mice (Fig. 7B).

In the control group, the architecture of the intestine is uniform, with the mucosa showing uneven swelling. The surface epithelium remains intact for the most part, although the apical portion of the villi is partially desquamated. The rest of the surface is composed of tall columnar enterocytes, with well-defined brush borders. The epithelial lining of the colon is preserved, with cells tightly packed together. The submucosa is composed of connective tissue with blood vessels. The intestinal villi correspond to the normal development of the organ (Fig. 8A), and the crypts are shallow and of regular shape (Fig. 8B).

In mice receiving MTX injections, there was uneven infiltration of lymphocytes and plasma cells, with a

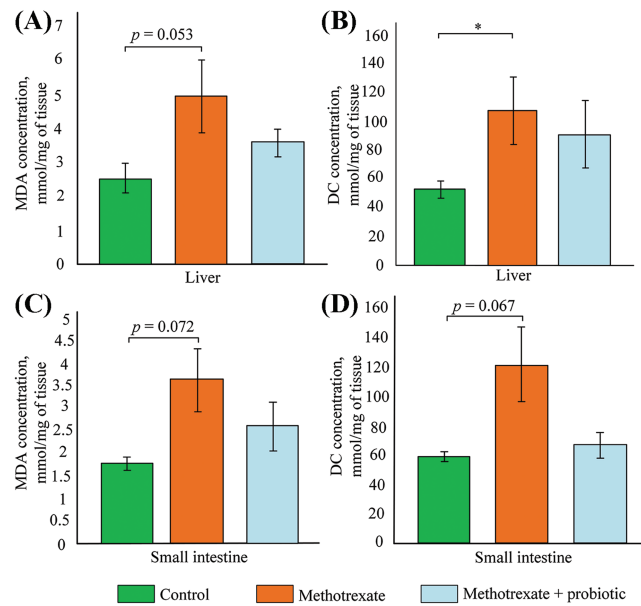


FIGURE 5. Effect of methotrexate (MTX) and probiotics on (A) malondialdehyde (MDA) concentration in the liver, (B) diene conjugates (DC) concentration in the liver, (C) MDA concentration in the small intestine, and (D) DC concentration in the small intestine. The control group of mice (n = 6), the MTX group (n = 8), and the MTX + probiotics group (n = 8). Differences between groups are statistically significant: * $p < 0.05$ (Kruskal-Wallis test).

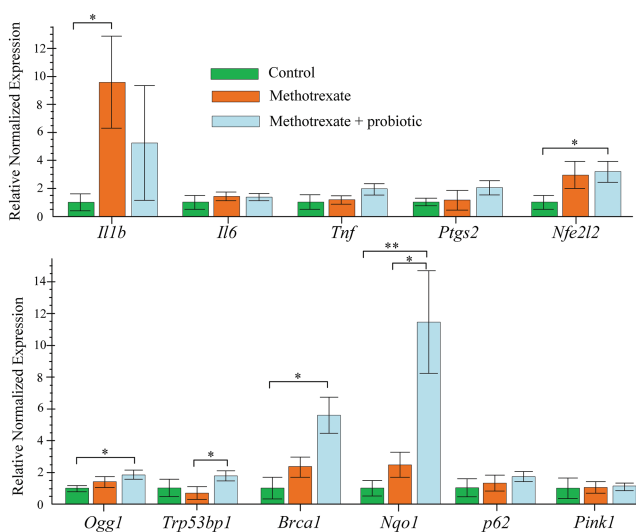


FIGURE 6. Effect of methotrexate (MTX) and probiotics on the level of gene expression in the small intestine of mice. The control group of mice (n = 6), the MTX group (n = 8), and the MTX + probiotics group (n = 8). Differences between groups are statistically significant: * $p < 0.05$, ** $p < 0.01$ (Kruskal-Wallis test).

moderate presence of neutrophils, scattered mostly in the villi. Desquamation of the epithelial layer was observed in the apical portion. The epithelial lining of the villi was disrupted with signs of infiltration (Fig. 9A). The submucosa consisted of connective tissue. The crypts in the small intestine are shallow, poorly branched, and exhibit low mitotic activity (Fig. 9B). This may indicate a compensatory reaction in the intestine following the administration of the drug.

Histological examination of the small intestine of the MTX + probiotics group revealed focal edema of the villi stroma, and congestion of blood vessels with a small

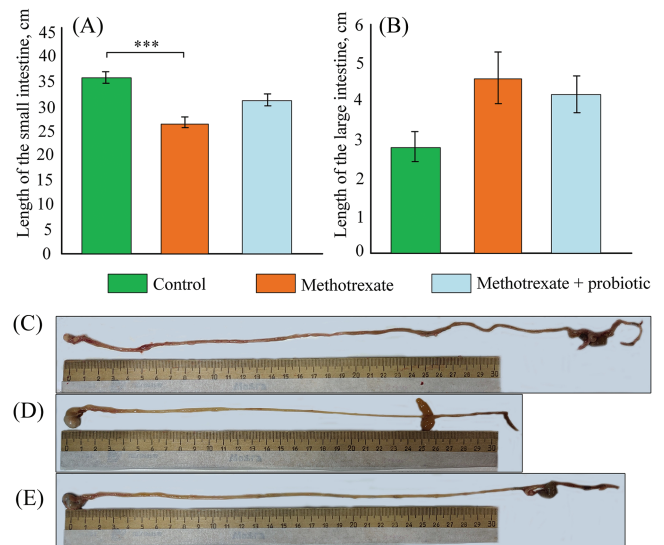


FIGURE 7. Effect of methotrexate (MTX) and probiotics on the length of the small intestine (A) and large intestine (B) in mice. Representative photos of the intestine in the control group of mice (C), mice receiving MTX injections (D), and mice receiving probiotics and MTX injections (E). The control group of mice (n = 6), the MTX group (n = 8), the MTX + probiotics group (n = 8). Differences between groups are statistically significant: *** $p < 0.001$ (Kruskal-Wallis test).

number of lymphocytes scattered within the stroma. The crypts were short, and moderately curved, with a large number of Paneth cells in the depths and intact epithelial lining throughout, along with rare mitotic figures within their epithelial layer (Fig. 10A). The intestinal epithelial lining remained intact, with tightly packed cells. The submucosa consisted of connective tissue, and focal infiltration was observed. The visualization of intestinal villi was also observed (Fig. 10B).

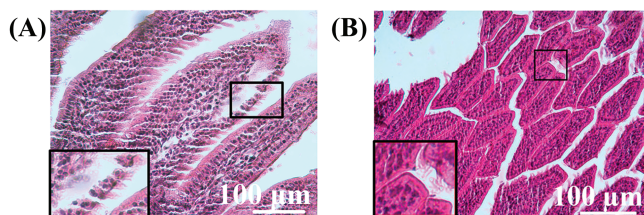


FIGURE 8. Morphological structure of the intestine in mice of the control group. (A) Intestinal villi, (B) crypts. Magnification A, B $\times 40$ hematoxylin-eosin staining.

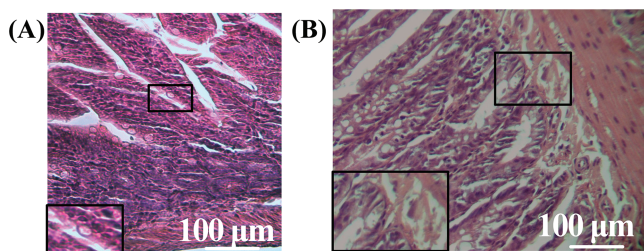


FIGURE 9. Morphological structure of the intestine in mice of the MTX group. (A) Tissue infiltration in villi, (B): crypts. Magnification A, B $\times 40$. Hematoxylin-eosin staining.

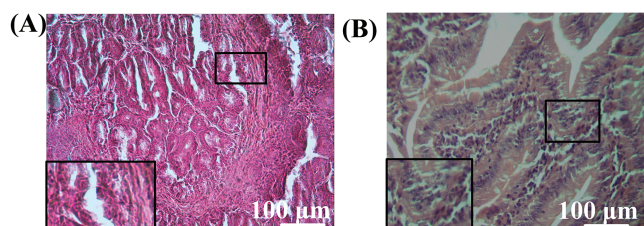


FIGURE 10. Morphological structure of the intestine of mice from the MTX + probiotics group. (A) Crypts, (B) intestine villi. Magnification: $\times 40$. Staining: Hematoxylin-eosin.

Discussion

Many cytotoxic drugs used in the therapy of oncological diseases are highly toxic to various components of mitochondria. Previously, our research group demonstrated that 50 μg of cisplatin in isolated kidney mitochondria doubled the amount of lipid peroxidation products and tripled the amount of mtDNA damage [7]. In this study, on the contrary, MTX caused a 3-fold increase in the intensity of lipid peroxidation in liver mitochondria at a concentration of 25 $\mu\text{g}/\text{mg}$ protein (Fig. 2), while a statistically significant increase in the number of mtDNA damage was observed only at a concentration of 37.5 $\mu\text{g}/\text{mg}$ protein (Fig. 2). This process may be related to the peculiarities of metabolism or the lipid profile of liver and kidney mitochondria. The differences in the toxicological effects of cisplatin and MTX could also be an important factor contributing to the distinct results. Cisplatin can exert an anticancer effect due to its ability to form coordination bonds in DNA between two purine bases and a platinum atom through alkylation. This leads to the formation of interstrand and intrastrand cross-links, which results in structural distortions in the DNA double helix and disruption of the DNA replication and transcription mechanisms [35]. However, it was shown by our research

group that cisplatin cannot directly increase the rate of production of ROS in mitochondria [7]. MTX can enhance oxidative stress, thereby participating in DNA structure damage. MTX is capable of inhibiting dihydrofolate reductase (DHFR). DHFR serves as a catalyst for the reduction of dihydrobiopterin to tetrahydrobiopterin, which in turn is necessary as a cofactor for the synthesis of nitric oxide (NO) by nitric oxide synthases (NOS). ROS increases when NOS are uncoupled due to the depletion of tetrahydrobiopterin reserves [8]. MTX contributes to the depletion of antioxidants, particularly GSH, which also significantly contributes to the increased intensity of oxidative damage [36]. Thus, it is likely that the increase in levels of mtDNA damage is also a consequence of oxidative stress rather than direct interaction of MTX with the mitochondrial genome.

The highest levels of mtDNA damage induced by intraperitoneal injections of MTX were observed in the liver (+98%, $p < 0.001$), blood (+86%, $p < 0.01$), and small intestine (+82%, $p < 0.001$) (Fig. 4C,G,I). The higher number of mtDNA damage in the liver can be explained by its role as the primary detoxifying organ, making it more susceptible to significant damage from various toxins and drugs. Additionally, the liver contains a substantial amount of lipids, and many drugs, including MTX, can increase the intensity of lipid peroxidation through induction of oxidative stress [37]. This is supported by our studies, where we found a twofold increase in the concentration of primary lipid peroxidation products (DC) (Fig. 5) and secondary lipid peroxidation products (MDA) (Fig. 5). We observed a significant increase in the levels of oxidative damage to mtDNA in the blood of mice receiving MTX injections (Fig. 4). This is consistent with data showing that patients undergoing uterine myoma therapy with MTX experienced a significant increase in genomic instability, manifested by an increase in the number of micronuclei in peripheral blood lymphocytes [38]. It is worth noting that in mice receiving probiotics along with MTX, the level of mtDNA damage did not differ from those mice receiving only MTX (Fig. 4I). Additionally, the level of lipid peroxidation products in the liver did not differ from control values, but there were also no significant differences compared to the group of mice receiving only MTX injections (Fig. 5). This suggests that the protective effect of probiotics against MTX-induced toxicity in the liver and blood is quite limited.

MTX adverse effects on the gastrointestinal tract, especially the small intestine, are notably severe. Our observations revealed a marked rise in MTX-induced mtDNA damage (Fig. 4) and a trend towards elevated levels of lipid peroxidation products in the small intestine (Fig. 5). These findings underscore MTX role in inducing substantial oxidative stress within small intestinal cells. It has been previously noted that MTX increases oxidative stress in various organs, including the brain. Oxidative stress under the influence of MTX can arise due to the induction of apoptosis caused by excessive production of ROS [39]. The administration of MTX caused a significant decrease in the levels of Nuclear factor erythroid 2-related factor 2 (Nrf2) and Heme oxygenase 1 (HO-1), which are protective factors against oxidative damage and inflammation. The

attenuation of the Nrf2/HO-1 pathway is a direct consequence of sustained generation of ROS induced by MTX [40]. Additionally, there is evidence that MTX induces renal oxidative stress, increasing the levels of MDA and NO, while decreasing the level of renal GSH [41]. The ability of MTX to increase the levels of ROS also induces a pro-inflammatory response, involving the activation of iNOS and TNF- α [42].

The oxidative disturbances were accompanied by histological changes. Firstly, it is worth noting that in mice receiving MTX, the length of the small intestine decreased by 19% ($p < 0.01$) compared to control mice (Fig. 7). The reduction in intestinal length may indicate certain pathologies of the gastrointestinal tract, particularly enteritis-inflammation in the small intestine, leading to changes in the mucous membrane [43]. It should also be noted that morphological examination of the intestine revealed structural changes in mice treated with MTX, characterized by leukocytic infiltration of the tissues in the intestine (Figs. 9,10).

Based on the data obtained, we can compare the conducted experiment with analogous studies Abdul-Wahab et al. [44] and Asoskova et al. [45], in which MTX exhibits strong anti-inflammatory activity, which, in our opinion, may account for the pathological changes in the small intestine. However, in the MTX + probiotics group (Fig. 10) of experimental mice, where a probiotic supplement was used, the dystrophic processes in the small intestine were less pronounced. In the study of Katturajan et al. [46], the quantitative composition of the intestinal microbiota was examined when using MTX, and it was found that the quantitative composition of the microbiota decreased when the drug was administered. Therefore, in our opinion, the probiotic supplement allowed for the stabilization of the microbiota and the mitigation of the toxic effects of the drug.

Previous studies have shown that MTX can induce villous atrophy and disrupt the epithelial architecture of the small intestine [47]. We also observed a significant decrease in body weight of mice immediately after the start of the intraperitoneal MTX injections (Fig. 3). This can be explained by the fact that MTX leads to the disruption of the intestinal barrier and digestive disturbances, thereby causing a range of gastrointestinal complications and poor nutrient absorption.

However, recent studies have shown that MTX treatment can be used for the therapy of intestinal diseases. It has been demonstrated that monotherapy with MTX at low doses (7.5–25.0 mg/week) administered orally and parenterally is sufficiently effective in patients with Crohn's disease. The rates of clinical remission were 76.3%, 74.6%, and 80.0% at 6, 12, and 24 months, respectively [48]. Currently, research has shown that MTX is effective in maintaining remission for up to one year in 25%–69% of children with Crohn's disease [49].

With intraperitoneal injections of MTX at a concentration of 5 mg/kg/day, on the contrary, we observed an increase in the expression level of *Il1b* in the small intestine (Fig. 6), which may indicate the activation of inflammatory processes. There is evidence that damage to the small intestine caused by MTX is accompanied by

increased expression of *Tnf- α* and Interleukin 1beta (*Il-1b*) genes, which play a role in inflammation processes [50].

Probiotics have been shown to have a protective effect against MTX-induced toxicity in the small intestine. It is known that certain strains of *Bifidobacterium* bacteria can produce mycosporine-like amino acids, which can impact the regulation of proliferation and differentiation of intestinal epithelial cells. Additionally, it has been shown that the consumption of a probiotics consisting of a mixture of *Lactobacillus* and *Bifidobacterium* strains increased the expression of tight junction proteins in the intestinal mucosa, improved its integrity, and reduced the number of enteropathogenic bacteria during the treatment of oncological diseases [51]. It has been shown that the use of *Bacteroides fragilis* reduces inflammation caused by MTX [29]. In our study, the level of the pro-inflammatory marker *Il1b* in the group of mice that received probiotics along with MTX did not statistically significantly increase compared to the control group (Fig. 6), which may indicate an anti-inflammatory effect of probiotics.

Moreover, it was found that in mice receiving probiotics along with MTX, the level of lipid peroxidation products in the small intestine did not increase relative to the control group (Fig. 5). Studies have shown that lactobacteria and bifidobacteria, as well as their cellular components, possess strong antioxidant properties [52]. For example, *Lactobacillus rhamnosus* has the ability to directly scavenge free radicals and inhibit the peroxidation of linoleic acid [53]. Probiotics have been found to exert an antioxidant effect at the level of gene transcription regulation. We discovered that in the small intestine of mice receiving probiotics along with MTX, the expression of the *Nfe2l2* gene (Fig. 6), which encodes the transcription factor Nrf2, was increased. The Nuclear factor erythroid 2-related factor 2/Antioxidant response element (Nrf2/ARE) signaling pathway is one of the main mechanisms by which cells adapt to oxidative stress, as it regulates the expression of many key antioxidant genes. Recent studies have shown that inflammatory bowel diseases can be alleviated through probiotics that act via the Nrf2 signaling pathway. *In vitro* studies have demonstrated that *Lactobacillus fermentum* Lf1 can enhance the expression of Nrf2 [54]. Deeper research has also shown that *Lactobacillus plantarum* P101 and *Lactobacillus rhamnosus* GG activated the Nrf2/ARE pathway *in vivo* to reduce hepatotoxicity induced by cyclophosphamide [55]. In another study, it was confirmed that *Lactobacillus plantarum* KSFY01 stimulates the activation of the Nrf2 pathway, and the expression level of Nrf2 increased proportionally with the dosage of the probiotic [56].

The Nrf2/ARE pathway is an activator of the *Nqo1* gene expression as it contains specific ARE sequences in its promoter region [57]. Indeed, Quinone oxidoreductase 1 (NQO1) plays a crucial role in protecting the intestine from damage. Studies have shown that mice with a knockout of the *Nqo1* gene have reduced levels of claudin and occludin, which are key molecules of the tight junctions of intestinal epithelial cells. Additionally, high levels of oxidative stress, as indicated by increased levels of ROS, were observed in these mice [58]. Downregulation of NQO1 impaired

mitochondrial function and mitochondrial antioxidant protection [59]. The antioxidant activity of NQO1 lies in its ability to catalyze the two-electron mediated reduction of quinones to hydroquinones. Normal one-electron reduction of quinones leads to the formation of an unstable semiquinone, which can donate an electron to oxygen, generating O_2^- . NQO1 generates a relatively stable hydroquinone while utilizing NAD(P)H during this process [60]. It is known that NQO1 reduces xenobiotics to less-reactive compounds via 2-electron reduction [61].

There is evidence that the consumption of apple puree containing the probiotic *L. plantarum* increased the level of Nrf2 in ischemic myocardium and induced Nrf2-regulated antioxidant enzymes such as HO-1 and NQO-1 [62]. Thus, we can assume that significant upregulation of NQO1 in the intestine (likely through an Nrf2-dependent manner), induced by probiotic therapy, may contribute significantly to the protection of the small intestine against MTX-induced damage.

Some lactobacilli have the ability to inhibit DNA breaks induced by peroxy radicals [63]. In our study, we found that the amount of mtDNA damage in the small intestine of mice receiving MTX in combination with probiotics was 26% lower ($p < 0.05$) compared to mice receiving only MTX. This could be attributed to the antioxidant properties of the probiotics as well as their ability to activate DNA repair pathways. We observed a significant expression of the *Ogg1*, *Trp53bp1*, and *Brcal* genes in the group of mice receiving MTX in combination with probiotics (Fig. 6). Oxoguanine glycosylase 1 (OGG1) is the primary glycosylase that removes 8-oxoG, the most common type of mtDNA damage that occurs as a result of oxidative stress or exposure to drugs and xenobiotics [64], including MTX. Specific inhibition of OGG1 in combination with the administration of MTX increased the extent of DNA damage [65]. However, in our study, probiotics, on the contrary, stimulated the expression of OGG1 (Fig. 6), which subsequently reduced the extent of mitochondrial genome damage.

OGG-1 contains an N-terminal mitochondrial targeting signal (MTS), which enables its transport into mitochondria. Therefore, OGG-1 can contribute to the protection of mtDNA from damage [66]. The OGG1 gene contains ARE, and a positive correlation between Nrf2 expression and OGG1 has been demonstrated [67]. There is evidence that breast cancer susceptibility gene 1 (BRCA1) contributes to maintaining the integrity of mtDNA. It is well-established that BRCA1 is involved in the regulation of glycosylases, including OGG1 [68]. There is a complex bidirectional regulatory system between Nrf2 and BRCA1. It has been shown that over-expression of Nrf2 stimulates BRCA1 expression [69]. In turn, BRCA1 can physically interact with Nrf2 and facilitate its nuclear translocation [70]. We also found that probiotics promote an increase in the expression of the *Trp53bp1* gene, which encodes the protein p53 binding protein 1 (53BP1) (Fig. 6). This enzyme has an important function in the repair of DNA double-strand breaks [71]. The presence of ARE-sequences in the promoter region of the *Trp53bp1* gene was previously detected in human colon epithelial cells [72]. Therefore, all

three genes studied (*Ogg1*, *Trp53bp1*, *Brcal*) have ARE sequences and can potentially be regulated by Nrf2. Thus, the protection of mtDNA in the small intestine from MTX-induced damage may be associated with the activation of repair systems through the Nrf2-dependent pathway, which is activated in small intestinal cells upon probiotic intake.

The main limitation of this study is that we can only speculate that the protective effect of probiotics is based on the activation of the Nrf2/ARE pathway. We do not provide irrefutable evidence for this assumption. Additional experiments are needed to assess the binding of transcription factors to the promoter regions of target genes, for example, using the chromatin immunoprecipitation (ChIP) method combined with high-throughput DNA sequencing (Seq) (ChIP-Seq method). Experiments on knockout mouse models (Nrf2^{-/-}) could also clarify our research.

Conclusion

Thus, we have demonstrated that MTX is highly toxic to liver mitochondria, leading to an increase in mtDNA damage and lipid peroxidation of membranes both *in vitro* and *in vivo*. Similar toxic effects were observed in the small intestine, accompanied by morphological changes in the intestine. The probiotic mixture partially mitigated the destructive processes induced by the course of MTX injections. We hypothesize that this may be due to the anti-inflammatory and antioxidant effects of probiotics, as well as their ability to modulate the activity of the Nrf2/ARE pathway. This signaling cascade regulates the expression of antioxidant genes, genes associated with drug and xenobiotic detoxification, as well as DNA repair systems. The comprehensive positive effect of the probiotic mixture opens up possibilities for their use in conjunction with MTX therapy to protect the intestine.

Acknowledgement: None.

Funding Statement: This research was carried out within the State Assignment of the Ministry of Science and Higher Education of the Russian Federation (project FZGW-2024-0003).

Author Contributions: The authors confirm contribution to the paper as follows: study conception and design: Artem P. Gureev, Anastasia V. Kokina; data collection: Ksenia S. Stafeeva, Olga A. Karandeeva, Veronika V. Nesterova, Natalia A. Samoylova, Kirill A. Starodubtsev, Evgeny S. Popov, Natalia S. Rodionova; analysis and interpretation of results: Natalia A. Samoylova, Veronika V. Nesterova, Evgeny V. Mikhailov, Ilya O. Krutov, Anastasia V. Kokina; draft manuscript preparation: Ksenia S. Stafeeva, Artem P. Gureev. All authors reviewed the results and approved the final version of the manuscript.

Availability of Data and Materials: The datasets generated and/or analyzed during the current study are available from the corresponding author on reasonable request.

Ethics Approval: The rearing, housing, and killing of mice was performed in accordance with the rules established by

the Ethical Committee for Biomedical Research of Voronezh State University (Section of Animal Care and Use, Minutes 42-03, 08 October 2020).

Conflicts of Interest: The authors declare no conflicts of interest to report regarding the present study.

References

- Byrne S, Boyle T, Ahmed M, Lee SH, Benyamin B, Hyppönen E. Lifestyle, genetic risk and incidence of cancer: a prospective cohort study of 13 cancer types. *Int J Epidemiol.* 2023;52(3): 817–26. doi:10.1093/ije/dyac238.
- Jiang H, Zuo J, Li B, Chen R, Luo K, Xiang X, et al. Drug-induced oxidative stress in cancer treatments: angel or devil? *Redox Biol.* 2023;63(Suppl 1):102754. doi:10.1016/j.redox.2023.102754.
- Chang L, Ruiz P, Ito T, Sellers WR. Targeting pan-essential genes in cancer: challenges and opportunities. *Cancer Cell.* 2021;39(4): 466–79. doi:10.1016/j.ccell.2020.12.008.
- Alfarhan M, Jafari E, Narayanan SP. Acrolein: a potential mediator of oxidative damage in diabetic retinopathy. *Biomolecules.* 2020;10(11):1579. doi:10.3390/biom10111579.
- Chen VC, Wu YF, Tsai YH, Weng JC. Association of longitudinal changes in cerebral microstructure with cognitive functioning in breast cancer survivors after adjuvant chemotherapy. *J Clin Med.* 2024;13(3):668. doi:10.3390/jcm13030668.
- Krutsikh EP, Potanina DV, Samoylova NA, Gryaznova MV, Sadovnikova IS, Gureev AP, et al. Brain protection by methylene blue and its derivative, azul B, via activation of the Nrf2/ARE pathway in cisplatin-induced cognitive impairment. *Pharmaceuticals.* 2022;15(7):815. doi:10.3390/ph15070815.
- Samoylova NA, Gureev AP, Popov VN. Methylene blue induces antioxidant defense and reparation of mitochondrial DNA in a Nrf2-dependent manner during cisplatin-induced renal toxicity. *Int J Mol Sci.* 2023;24(7):6118. doi:10.3390/ijms24076118.
- Bedoui Y, Guillot X, Sélambarom J, Guiraud P, Giry C, Jaffar-Bandjee MC, et al. Methotrexate an old drug with new tricks. *Int J Mol Sci.* 2019;20(20):5023. doi:10.3390/ijms20205023.
- Genestier L, Paillet R, Quemeneur L, Izeradjene K, Revillard JP. Mechanisms of action of methotrexate. *Immunopharmacology.* 2000;47(2–3):247–57. doi:10.1016/S0162-3109(00)00189-2.
- Hamilton BK, Rybicki LA, Li H, Lucas T, Corrigan D, Kalaycio M, et al. Tacrolimus/methotrexate vs tacrolimus/reduced-dose methotrexate/mycophenolate for graft-versus-host disease prevention. *Blood Adv.* 2023;7(16):4505–13. doi:10.1182/bloodadvances.2023010310.
- Kozmiński P, Halik PK, Chesori R, Gniazdowska E. Overview of dual-acting drug methotrexate in different neurological diseases, autoimmune pathologies and cancers. *Int J Mol Sci.* 2020;21(10): 3483. doi:10.3390/ijms21103483.
- Ismail MD, Wiratnaya IGE, Raditya RH. Evaluating the outcome and patient safety of methotrexate, doxorubicin, and cisplatin regimen for chemotherapy in osteosarcoma: a meta-analysis. *Asian Pac J Cancer Prev.* 2024;25(5):1497–505. doi:10.31557/APJCP.2024.25.5.1497.
- Xu J, Xiao L, Zhu J, Qin Q, Fang Y, Zhang JA. Methotrexate use reduces mortality risk in rheumatoid arthritis: a systematic review and meta-analysis of cohort studies. *Semin Arthritis Rheum.* 2022;55(Suppl 3):152031. doi:10.1016/j.semarthrit.2022.152031.
- Wasko MC, Dasgupta A, Hubert H, Fries JF, Ward MM. Propensity-adjusted association of methotrexate with overall survival in rheumatoid arthritis. *Arthritis Rheum.* 2013;65(2): 334–42. doi:10.1002/art.37723.
- Herfarth HH, Long MD, Isaacs KL. Methotrexate: underused and ignored? *Dig Dis.* 2012;30(Suppl 3):112–8. doi:10.1159/000342735.
- Sahu K, Langeh U, Singh C, Singh A. Crosstalk between anticancer drugs and mitochondrial functions. *Curr Res Pharmacol Drug Discov.* 2021;2(3):100047. doi:10.1016/j.crphar.2021.100047.
- Li P, Inoue Y, Miyamoto D, Adachi T, Okada S, Adachi T, et al. Therapeutic effect and mechanism of daikenchuto in a model of methotrexate-induced acute small intestinal mucositis. *PLoS One.* 2023;18(3):e0283626. doi:10.1371/journal.pone.0283626.
- Schmidt S, Messner CJ, Gaiser C, Hämmerli C, Suter-Dick L. Methotrexate-induced liver injury is associated with oxidative stress, impaired mitochondrial respiration, and endoplasmic reticulum stress *in vitro*. *Int J Mol Sci.* 2022;23(23):15116. doi:10.3390/ijms232315116.
- Yanaşoğlu E, Büyükavcı M, Çetinkaya A, Turan G, Koroğlu M, Yazar H, et al. Silibinin effect on methotrexate-induced hepatotoxicity in rats. *Eurasian J Med.* 2022;54(3):264–9. doi:10.5152/eurasianjmed.2022.20371.
- Aboubakr EM, Ibrahim ARN, Ali FEM, Mourad AAE, Ahmad AM, Hofni A. Fasudil ameliorates methotrexate-induced hepatotoxicity by modulation of redox-sensitive signals. *Pharmaceuticals.* 2022;15(11):1436. doi:10.3390/ph15111436.
- Ting NL, Lau HC, Yu J. Cancer pharmacomicrobiomics: targeting microbiota to optimise cancer therapy outcomes. *Gut.* 2022;71(7):1412–25. doi:10.1136/gutjnl-2021-326264.
- Badgeley A, Anwar H, Modi K, Murphy P, Lakshmikuttyamma A. Effect of probiotics and gut microbiota on anti-cancer drugs: mechanistic perspectives. *Biochim Biophys Acta Rev Cancer.* 2021;1875(1):188494. doi:10.1016/j.bbcan.2020.188494.
- Sharaf LK, Sharma M, Chandel D, Shukla G. Prophylactic intervention of probiotics (*L. acidophilus*, *L. rhamnosus* GG) and celecoxib modulate Bax-mediated apoptosis in 1,2-dimethylhydrazine-induced experimental colon carcinogenesis. *BMC Cancer.* 2018;18(1):1111. doi:10.1186/s12885-018-4999-9.
- Tian Y, Li M, Song W, Jiang R, Li YQ. Effects of probiotics on chemotherapy in patients with lung cancer. *Oncol Lett.* 2019;17(3):2836–48. doi:10.3892/ol.2019.9906.
- Reyna-Figueroa J, Barrón-Calvillo E, García-Parra C, Galindo-Delgado P, Contreras-Ochoa C, Lagunas-Martínez A, et al. Probiotic supplementation decreases chemotherapy-induced gastrointestinal side effects in patients with acute leukemia. *J Pediatr Hematol Oncol.* 2019;41(6):468–72. doi:10.1097/MPH.0000000000001497.
- Mi H, Dong Y, Zhang B, Wang H, Peter CCK, Gao P, et al. Bifidobacterium infantis ameliorates chemotherapy-induced intestinal mucositis via regulating T cell immunity in colorectal cancer rats. *Cell Physiol Biochem.* 2017;42(6):2330–41. doi:10.1159/000480005.
- Bowen JM, Stringer AM, Gibson RJ, Yeoh AS, Hannam S, Keefe DM. VSL#3 probiotic treatment reduces chemotherapy-induced diarrhea and weight loss. *Cancer Biol Ther.* 2007;6(9):1449–54. doi:10.4161/cbt.6.9.4622.
- Linn YH, Thu KK, Win NHH. Effect of probiotics for the prevention of acute radiation-induced diarrhoea among

- cervical cancer patients: a randomized double-blind placebo-controlled study. *Probiotics Antimicrob Proteins*. 2019; 11(2):638–47. doi:10.1007/s12602-018-9408-9.
29. Zhou B, Xia X, Wang P, Chen S, Yu C, Huang R, et al. Induction and amelioration of methotrexate-induced gastrointestinal toxicity are related to immune response and gut microbiota. *eBioMedicine*. 2018;33(Suppl. 2):122–33. doi:10.1016/j.ebiom.2018.06.029.
 30. Lowry OH, Rosebrough NJ, Farr AL, Randall RJ. Protein measurement with the Folin phenol reagent. *J Biol Chem*. 1951;193(1):265–75.
 31. Gureev AP, Sadovnikova IS, Chernyshova EV, Tsvetkova AD, Babenkova PI, Nesterova VV, et al. Beta-hydroxybutyrate mitigates sensorimotor and cognitive impairments in a photothrombosis-induced ischemic stroke in mice. *Int J Mol Sci*. 2024;25(11):5710. doi:10.3390/ijms25115710.
 32. Xue R, Du M, Zhou TY, Ai WZ, Zhang ZS, Xiang XW, et al. Polysaccharides from hemp seed protect against cyclophosphamide-induced intestinal oxidative damage via Nrf2-Keap1 signaling pathway in mice. *Oxid Med Cell Longev*. 2020;2020(12):1813798–13. doi:10.1155/2020/1813798.
 33. Antipova LV, Suleymanov SM, Slobodyanik VS. *Anatomy and histology of farm animals: textbook and workshop*. Moscow: Yurayt Publishing House; 2020.
 34. Al-Fawaeir S, Akgül E, Caycı T, Demirin H, Kurt Y, Aydın I, et al. Comparison of two methods for malondialdehyde measurement. *J Clin Anal Med*. 2011;2(2):2–4. doi:10.4328/JCAM.209.
 35. de Biasi AR, Villena-Vargas J, Adusumilli PS. Cisplatin-induced antitumor immunomodulation: a review of preclinical and clinical evidence. *Clin Cancer Res*. 2014;20(21):5384–91. doi:10.1158/1078-0432.CCR-14-1298.
 36. Katturajan R, Vijayalakshmi S, Rasool M, Prince SE. Molecular toxicity of methotrexate in rheumatoid arthritis treatment: a novel perspective and therapeutic implications. *Toxicology*. 2021;461:152909. doi:10.1016/j.tox.2021.152909.
 37. Ghoneum M, El-Gerbed MSA. Human placental extract ameliorates methotrexate-induced hepatotoxicity in rats via regulating antioxidative and anti-inflammatory responses. *Cancer Chemother Pharmacol*. 2021;88(6):961–71. doi:10.1007/s00280-021-04349-4.
 38. Novakovic T, Milosevic-Djordjevic OM, Grujicic DV, Marinkovic DM, Jankovic S, Arsenijevic SN. Effect of intratumoral application of methotrexate *in vivo* on frequency of micronuclei in peripheral blood lymphocytes. *Arch Oncol*. 2003;11(1):1–4. doi:10.2298/AOO0301001N.
 39. Aslankoc R, Savran M, Doğuç DK, Sevimli M, Tekin H, Kaynak M. Ameliorating effects of ramelteon on oxidative stress, inflammation, apoptosis, and autophagy markers in methotrexate-induced cerebral toxicity. *Iran J Basic Med Sci*. 2022;25(10):1183–9. doi:10.22038/IJBMS.2022.62955.13913.
 40. Younis NS, Elsewedy HS, Shehata TM, Mohamed ME. Geraniol averts methotrexate-induced acute kidney injury via Keap1/Nrf2/HO-1 and MAPK/NF- κ B pathways. *Curr Issues Mol Biol*. 2021;43(3):1741–55. doi:10.3390/cimb43030123.
 41. Aldossary SA, Chohan MS, Mohaini MA, Tasleem Rasool S. Capsaicin ameliorate the nephrotoxicity induced by methotrexate. *Pak J Pharm Sci*. 2021;34(6):2191–5.
 42. Morsy MA, Abdel-Latif R, Hafez SMNA, Kandeel M, Abdel-Gaber SA. Paeonol protects against methotrexate hepatotoxicity by repressing oxidative stress, inflammation, and apoptosis-the role of drug efflux transporters. *Pharmaceuticals*. 2022;15(10):1296. doi:10.3390/ph15101296.
 43. Xu H, Cai F, Li P, Wang X, Yao Y, Chang X, et al. Characterization and analysis of the temporal and spatial dynamic of several enteritis modeling methodologies. *Front Immunol*. 2021;12:727664. doi:10.3389/fimmu.2021.727664.
 44. Abdul-Wahab FK, Al-Shawi NN. Effects of vitamin D3 on methotrexate-induced jejunum damage in rats. *Iraqi J Pharm Sci*. 2020;29(1):260–7.
 45. Asoskova A, Sychev D, Kubanov A. Methotrexate safety in psoriasis: an overview. *Ann Russ Acad Med Sci*. 2021;7(3): 254–67. doi:10.15690/vramn1527.
 46. Katturajan R, Prince SE. L-carnitine and zinc supplementation impedes intestinal damage in methotrexate-treated adjuvant-induced arthritis rats: reinstating enterocyte proliferation and trace elements. *J Trace Elem Med Biol*. 2023;78:127188. doi:10.1016/j.jtemb.2023.127188.
 47. Yamamoto T, Machida T, Tanno C, Hasebe S, Tamura M, Kobayashi N, et al. Low-dose nifedipine ameliorates tissue injury and inhibits 5-hydroxytryptamine synthesis in the rat intestine after methotrexate administration. *J Pharmacol Sci*. 2023;152(2):90–102. doi:10.1016/j.jphs.2023.03.005.
 48. Park J, Chun J, Park SJ, Park JJ, Kim TI, Yoon H, et al. Effectiveness and tolerability of methotrexate monotherapy in Crohn's disease patients: a multicenter observational study. *Therap Adv Gastroenterol*. 2023;16:17562848231191664. doi:10.1177/17562848231191664.
 49. Temtem TA, Vickers M, Whitworth J. Weekly folic acid is a convenient and well-tolerated alternative to daily dosing in pediatric patients with inflammatory bowel disease on methotrexate. *Nutrients*. 2023;15(7):1586. doi:10.3390/nu15071586.
 50. Ozcicek A, Cetin N, Keskin Cimen F, Tumkaya L, Malkoc I, Gulaboglu M, et al. The impact of resveratrol on oxidative stress induced by methotrexate in rat ileum tissue: evaluation of biochemical and histopathological features and analysis of gene expression. *Med Princ Pract*. 2016;25(2):181–6. doi:10.1159/000442020.
 51. Sánchez-Alcoholado L, Ramos-Molina B, Otero A, Laborda-Illanes A, Ordóñez R, Medina JA, et al. The role of the gut microbiome in colorectal cancer development and therapy response. *Cancers*. 2020;12(6):1406. doi:10.3390/cancers12061406.
 52. Averina OV, Poluektova EU, Marsova MV, Danilenko VN. Biomarkers and utility of the antioxidant potential of probiotic lactobacilli and bifidobacteria as representatives of the human gut microbiota. *Biomedicines*. 2021;9(10):1340. doi:10.3390/biomedicines9101340.
 53. Xing J, Wang G, Zhang Q, Liu X, Gu Z, Zhang H, et al. Determining antioxidant activities of lactobacilli cell-free supernatants by cellular antioxidant assay: a comparison with traditional methods. *PLoS One*. 2015;10(3):e0119058. doi:10.1371/journal.pone.0119058.
 54. Li B, Wang Y, Jiang X, Du H, Shi Y, Xiu M, et al. Natural products targeting Nrf2/ARE signaling pathway in the treatment of inflammatory bowel disease. *Biomed Pharmacother*. 2023;164(849–860):114950. doi:10.1016/j.biopha.2023.114950.
 55. You T, Zhao Y, Liu S, Xu H. Lactiplantibacillus plantarum P101 attenuated cyclophosphamide-induced liver injury in mice by regulating the Nrf2/ARE signaling pathway. *Int J Mol Sci*. 2023;24(17):13424. doi:10.3390/ijms241713424.
 56. Chen Q, Liu C, Zhang Y, Wang S, Li F. Effect of lactobacillus plantarum KSFY01 on the exercise capacity of D-galactose-induced oxidative stress-aged mice. *Front Microbiol*. 2022;13:1030833. doi:10.3389/fmicb.2022.1030833.

57. Venugopal R, Jaiswal AK. Nrf1 and Nrf2 positively and c-Fos and Fra1 negatively regulate the human antioxidant response element-mediated expression of NAD(P)H: quinone oxidoreductase1 gene. *Proc Natl Acad Sci U S A*. 1996; 93(25):14960–5. doi:10.1073/pnas.93.25.14960.
58. Nam ST, Hwang JH, Kim DH, Park MJ, Lee IH, Nam HJ, et al. Role of NADH: quinone oxidoreductase-1 in the tight junctions of colonic epithelial cells. *BMB Rep*. 2014;47(9):494–9. doi:10.5483/BMBRep.2014.47.9.196.
59. Wu YL, Wang D, Peng XE, Chen YL, Zheng DL, Chen WN, et al. Epigenetic silencing of NAD(P)H: quinone oxidoreductase 1 by hepatitis B virus X protein increases mitochondrial injury and cellular susceptibility to oxidative stress in hepatoma cells. *Free Radic Biol Med*. 2013;65(Suppl. 1):632–44. doi:10.1016/j.freeradbiomed.2013.07.037.
60. Ross D, Siegel D. Functions of NQO1 in cellular protection and CoQ10 metabolism and its potential role as a redox sensitive molecular switch. *Front Physiol*. 2017;8:595. doi:10.3389/fphys.2017.00595.
61. Gray JP, Karandrea S, Burgos DZ, Jaiswal AA, Heart EA. NAD (P)H-dependent quinone oxidoreductase 1 (NQO1) and cytochrome P450 oxidoreductase (CYP450OR) differentially regulate menadione-mediated alterations in redox status, survival and metabolism in pancreatic β -cells. *Toxicol Lett*. 2016;262:1–11. doi:10.1016/j.toxlet.2016.08.021.
62. Aboulgheit A, Karbasiafshar C, Zhang Z, Sabra M, Shi G, Tucker A, et al. Lactobacillus plantarum probiotic induces Nrf2-mediated antioxidant signaling and eNOS expression resulting in improvement of myocardial diastolic function. *Am J Physiol Heart Circ Physiol*. 2021;321(5):H839–49. doi:10.1152/ajpheart.00278.2021.
63. Vougiouklaki D, Tsironi T, Tsantes AG, Tsakali E, Van Impe JFM, Houhoula D. Probiotic properties and antioxidant activity *in vitro* of lactic acid bacteria. *Microorganisms*. 2023;11(5): 1264. doi:10.3390/microorganisms11051264.
64. Zhao F, Zhu J, Shi L, Wu X. OGG1 in the kidney: beyond base excision repair. *Oxid Med Cell Longev*. 2022;2022(9887): 5774641. doi:10.1155/2022/5774641.
65. Baquero JM, Benítez-Buelga C, Rajagopal V, Zhenjun Z, Torres-Ruiz R, Müller S, et al. Small molecule inhibitor of OGG1 blocks oxidative DNA damage repair at telomeres and potentiates methotrexate anticancer effects. *Sci Rep*. 2021;11(1):3490. doi:10.1038/s41598-021-82917-7.
66. Prakash A, Doublé S. Base excision repair in the mitochondria. *J Cell Biochem*. 2015;116(8):1490–9.
67. Amirinejad R, Shirvani-Farsani Z, Naghavi Gargari B, Sahraian MA, Mohammad Soltani B, Behmanesh M. Vitamin D changes expression of DNA repair genes in the patients with multiple sclerosis. *Gene*. 2021;781(10):145488. doi:10.1016/j.gene.2021.145488.
68. Saha T, Rih JK, Roy R, Ballal R, Rosen EM. Transcriptional regulation of the base excision repair pathway by BRCA1. *J Biol Chem*. 2010;285(25):19092–105. doi:10.1074/jbc.M110.104430.
69. Wang Q, Li J, Yang X, Sun H, Gao S, Zhu H, et al. Nrf2 is associated with the regulation of basal transcription activity of the BRCA1 gene. *Acta Biochim Biophys Sin*. 2013;45(3):179–87. doi:10.1093/abbs/gmt001.
70. Xu P, Liu Q, Xie Y, Shi X, Li Y, Peng M, et al. Breast cancer susceptibility protein 1 (BRCA1) rescues neurons from cerebral ischemia/reperfusion injury through NRF2-mediated antioxidant pathway. *Redox Biol*. 2018;18(10069):158–72. doi:10.1016/j.redox.2018.06.012.
71. Mirman Z, de Lange T. 53BP1: a DSB escort. *Genes Dev*. 2020; 34(1–2):7–23. doi:10.1101/gad.333237.119.
72. Kim SB, Pandita RK, Eskiocak U, Ly P, Kaisani A, Kumar R, et al. Targeting of Nrf2 induces DNA damage signaling and protects colonic epithelial cells from ionizing radiation. *Proc Natl Acad Sci U S A*. 2012;109(43):E2949–55. doi:10.1073/pnas.1207718109.